Estudo do magnetismo do nível 5d do Re em perovskitas duplas A_2FeReO_6 (A=Ca,Ba)

Aluna: Carla Azimonte
Orientador.: Eduardo Granado

Resumo

Em perovskitas duplas ordenadas, cuja fórmula é dada por $A_2B'B''O_6$ (onde A é um alcalino terroso ou um terra rara),os sítios dos metais de transição são ocupados alternativamente por diferentes cátions B' e B''. Desta família, os compostos A_2FeReO_6 e A_2FeMoO_6 (A= Ca, Sr, Ba) tem atraído interesse científico e tecnológico devido à magnetorresistência gigante observada à temperatura ambiente.

A maior parte dos compostos pertencentes a esta família, tais como Ba_2FeReO_6, Ba_2FeMoO_6 e Ca_2FeMoO_6, apresentam características ferrimagnéticas e metálicas. Porém, o composto Ca_2FeReO_6 apresenta uma característica única, pois além ser ferrimagnético, apresenta comportamento não metalíco.

A simetria do cristal Ca_2FeReO_6 é monoclínica, assim como a do Ca_2FeMoO_6, que é metálico. Neste cristal, o ângulo da ligação Fe-O-Re é muito menor do que o existente em Sr_2FeReO_6. Sabe-se que para perovskitas de metais de transição a distorção do ângulo de ligação reduz a energia de transferência dos elétrons do nível d ou a largura de banda de um elétron devido à redução da hibridização entre o estado d do metal de transição e o estado p do oxigênio. De fato, a variação do ângulo de ligação com a substituição do íon A ocasiona grandes mudanças eletrônicas, tais como uma magnetorresistência colossal e o controle da largura de banda da transição Mott. Sendo assim, pode-se concluir que o fenômeno metal-isolante (M-I) que aparece na família das perovskitas duplas é devido aos efeitos na estrutura induzidos pela substituição do Ca assim como pela mudança da configuração eletrônica entre o Mo e Re.

Neste projeto, foi realizado o estudo qualitativo do dicroísmo magnético do Re em Ca_2FeReO_6, utilizando a linha de luz DXAS (espectroscopia de absorção de raio-X dispersiva).

A partir dos dados obtidos foi possível verificar a existência de uma transição de fase em torno de 150K, verificamos também a forma com que a magnetização da amostra varia com o campo aplicado à ela, com isso, foi possível determinar o campo de saturação, necessário para magnetizar completamente a amostra.

Obtivemos sinal de dicroismo nas bordas L_2 e L_3 do Re, fato que indica a existência de um momento magnético do Re.

Introdução

Fenômenos recentes causados por elétrons localizados em estados orbitais degenerados tem sido um importante problema dos óxidos dos metais de transição nos últimos anos.

Para sistemas orbitais e_g, a degenerescência sobre o campo cristalino cúbico é freqüentemente removida por grandes distorções de Jahn-Teller do octaedro do oxigênio. A física dos elétrons localizados nos orbitais t_{2g} parcialmente ocupados é um pouco diferente, devido ao acoplamento relativo mais fraco de Jahn-Teller, à alta degenerescência e as simetrias adicionais dos orbitais t_{2g}.. Além disso, esses elétrons devem ter um momento magnético orbital não extinto e um acoplamento spin-orbita relevante.

Os estudos de Mossbauer em Ca_2FeReO_6 indicaram a presença de íons Fe^{3+}, então, o estado de oxidação dos íons do Re devem ser 5+, com dois elétrons no orbital 5d t_{2g}.

As estruturas nucleares e magnéticas, já estudadas em pesquisas anteriores, mostram fenômenos interessantes, tal como a existência de um acoplamento spin-orbita o qual revela a existência de magnetismo orbital.[i]

Embora esse acoplamento tenha sido detectado, a natureza precisa do momento magnético ~1muB/Mn do Re é ainda desconhecida.

Dicroísmo magnético circular de raio-X é particularmente útil para separar o momento magnético de spin do orbital em compostos ferro ou ferrimagnéticos.

Para metais de transição com magnetismo nos níveis atômicos d, as transições L2,3 (2p para 3d, 4d ou 5d) mostram os efeitos do dicroísmo mais fortemente pois o estado final é magnético. As energias dessas transições são muito baixas para os elementos 3d (<1kev), sendo assim, medidas utilizando absorção direta não podem ser feitas. Métodos de detecção indireta, usadas para estas energias, tal como o de rendimento total de elétrons introduzem complicações adicionais na análise dos dados, portanto as regras de soma usadas para extrair os momentos magnéticos orbital e de spin , a partir de dicroísmo magnético nas bordas L2,3, não são diretamente aplicáveis.

Por outro lado, tem-se as bordas L2,3 dos elementos 5d as quais estão na região do raio-X duro, em principio estes íons não são magnéticos devido as correlações eletrônicas fracas dos orbitais 5d.

Então, o magnetismo 5d do Re é muito interessante devido ao fato deste ser o único caso em que há um magnetismo 5d em um material "bulk" não diluído.

A linha DXAS é apropriada para este tipo de estudo, já que, espera-se que o sinal de dicroísmo para o Re na borda L seja muito mais forte do que para o metal de transição 3d na borda K ou dos terras raras (4f) na borda L na região do raio-X duro, onde o estado final é não magnético, exceto para os pequenos efeitos de hibridização.

A linha de luz dispersiva para absorção de raios-X[ii]

A linha de luz que utilizaremos (DXAS) tem algumas características interessantes, ela utiliza um único cristal, que uma vez curvado, permite a obtenção de um feixe de raio-X policromático, com uma largura de banda suficiente para a medida simultânea de todas as energias de um espectro de absorção completo, com isso o tempo de obtenção de um espectro é muito pequeno.

Com esse tipo de óptica dispersiva, cada região do cristal difrata o feixe com uma energia diferente, uma vez que a energia do feixe difratado depende do ângulo de incidência do feixe sobre o cristal, de acordo com a lei de Bragg

$$n\lambda = 2d \operatorname{sen} \theta_B$$

onde λ é o comprimento de onda, d é a distancia entre os planos cristalinos utilizados na monocromatização, θ_B é o ângulo entre o feixe incidente e os planos cristalinos. Além disso a energia E do feixe difratado se relaciona com λ, a constante de Planck h e a velocidade da luz no vácuo c da seguinte forma

$$E = \frac{hc}{\lambda}$$

Dessa forma, para cada ponto de incidência do feixe de raio-X sobre o cristal, teremos a lei de Bragg sendo satisfeita para uma diferente energia.

A curvatura do cristal também ocasiona a focalização do feixe refletido, permitindo que se obtenha tamanhos de feixe bem reduzidos, e uma boa resolução em energia. Essa

resolução é muito importante para medidas próximas à borda de absorção, pois neste caso os detalhes que devemos observar (largura de picos, ou posição de energia da borda de absorção) podem ser da ordem de décimos de eletron-volts.

A amostra Ca_2FeReO_6

Em perovskita dupla ordenada, cuja fórmula é dada por $A_2B'B''O_6$ (onde A é um alcalino terroso ou um terra rara),os sítios dos metais de transição são ocupados alternadamente por diferentes cátions B' e B''.

A maior parte dos compostos pertencentes a esta família, tais como Ba_2FeReO_6 (figura1), Ba_2FeMoO_6 e Ca_2FeMoO_6, apresentam características ferrimagnéticas e metálicas. Porém, existe o composto Ca_2FeReO_6 (figura2), que apresenta característica única, pois além de ser ferrimagnético, também apresenta comportamento não metálico.

Pode-se averiguar um comportamentos anômalo dos parâmetros da estrutura à temperaturas abaixo de Tc. A partir de medidas de difração de nêutron em pó, encontra-se que abaixo de ~300K e ~160K, a estrutura cristalina monoclínica separa em outras 2 ou 3 fases monoclínicas, respectivamente.

Quando um campo magnético é aplicado, há uma redução das fases adicionais à baixa temperatura em favor da fase à alta temperatura. Essas manifestações do grau de liberdade orbital dos elétrons do Re indicam que esses elétrons são fortemente correlacionados e que o composto é um isolante de Mott com competição entre estados de spin orbitalmente ordenados.[i]

A simetria do cristal Ca_2FeReO_6 é monoclínica, assim como a do Ca_2FeMoO_6 que é metálico. Neste cristal, o ângulo da ligação Fe-O-Re é aproximadamente 156°, muito menor do que o existente em Sr_2FeReO_6. Sabe-se que para perovskitas de metais de transição a distorção do ângulo de ligação reduz a energia de transferência dos elétrons do nível d ou a largura de banda de um elétron devido à redução da hibridização entre o estado d do metal de transição e o estado p do oxigênio[iii].

De fato, a variação do ângulo de ligação com a substituição do íon A ocasiona grandes mudanças eletrônicas, tais como uma magnetorresistência colossal e o controle da largura de banda da transição Mott.

Sendo assim, pode-se concluir que o fenômeno metal-isolante (M-I) que aparece na família das perovskitas duplas é devido aos efeitos na estrutura induzidos pela substituição do Ca assim como pela mudança da configuração eletrônica entre o Mo e Re. Isso também revela que as perovskitas duplas de base Fe,Re estão na borda de uma transição metal-isolante.

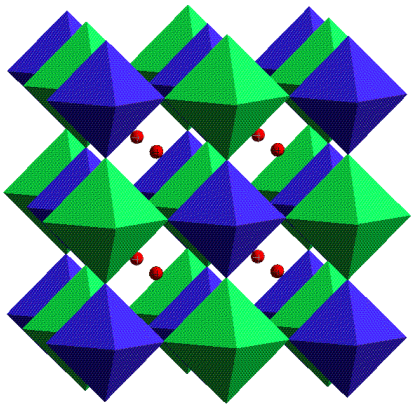

Fig1. Estrutura cristalina do composto Ba_2FeReO_6, onde os octaedros representam os átomos de oxigênio nos vértices e os átomos de Re e Fe no centro, alternadamente no azul e no verde, e as esferas vermelhas representam os átomos de Ba.

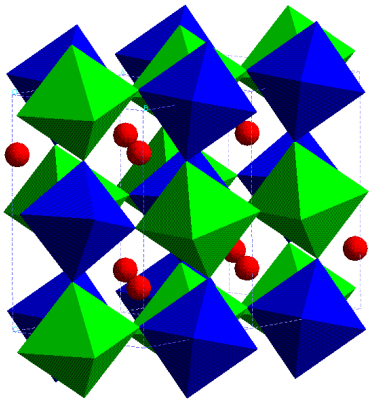

Fig2. Estrutura cristalina do composto Ca_2FeReO_6, onde os octaedros representam os átomos de oxigênio nos vértices e os átomos de Re e Fe no centro, alternadamente no azul e no verde, e as esferas vermelhas representam os átomos de Ca.

Dicroísmo Circular Magnético de raios-X[iv]

Os materiais magnéticos, quando iluminados com raios X absorvem de forma diferente a luz circularmente polarizada à direita daquela cicularmente polarizada à esquerda, se existir uma componente da magnetização paralela à direção de propagação dos fótons. Essa diferença é chamada de dicroísmo circular magnético.

Por exemplo, em uma amostra ferromagnetica ou ferrimagnética, o coeficiente de atenuação deve ser diferente com a luz incidente circularmente polarizados em um sentido ou no outro.

Em sistemas magnéticos reais, a magnetização é devida tanto à polarização orbital, quanto de spin. Por este motivo medidas de dicroísmo circular magnéticos podem fornecer dados sobre os momentos magnéticos orbital e de spin da amostra.

Na região do raio-X, os efeitos são realmente significantes quando muito próximos das bordas de absorção ressonantes, onde os fotoelétrons excitados sentem, fortemente, a presença do campo elétrico da amostra, e por conseqüência, o sinal obtido numa medida do coeficiente de absorção fica mais intenso. Por esse motivo, as medidas de dicroísmo magnético são feitas perto das bordas de absorção do material a ser estudado.

Dados obtidos

Primeiramente, para melhor entendimento dos dados de dicroismo obtidos, estudamos as características básicas das propriedades magnéticas da nossa amostra realizando medidas da magnetização em função da temperatura e em função do campo magnético aplicado, como podemos ver nos gráficos 1 e 2, respectivamente. Utilizamos para isso um magnetômetro MPMS, o qual está localizado no Grupo de Propriedades Ópticas e Magnéticas de sólidos (GPOMS) no Departamento de Eletrônica Quântica (DEQ) da Unicamp.

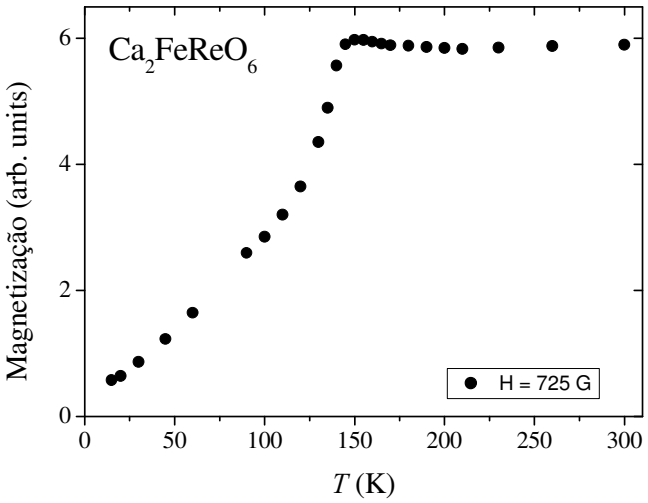

Gráfico 1: Medidas da magnetização da amostra de Ca_2FeReO_6 em função da temperatura utilizando um campo magnético aplicado de 725 Gauss.

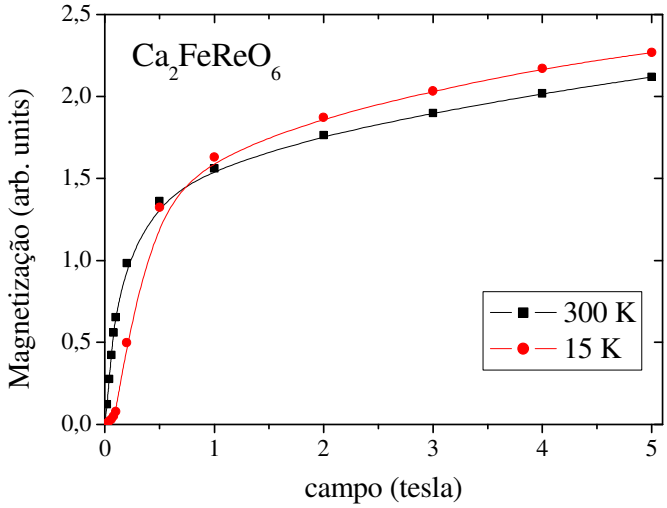

Gráfico 2: Medidas da magnetização da amostra de Ca_2FeReO_6 em função do campo magnético aplicado.

Realizando medidas de dicroismo magnético para a amostra de Ca_2FeReO_6 utilizando a linha de luz dispersiva para absorção de raios-X, obtivemos sinal de dicroismo em função de pixel para a borda L_3 e L_2 do Re, como mostrado nos gráficos 3 e 4, respectivamente. A escala do eixo x para os gráficos será modificada de pixel para uma escala em energia futuramente.

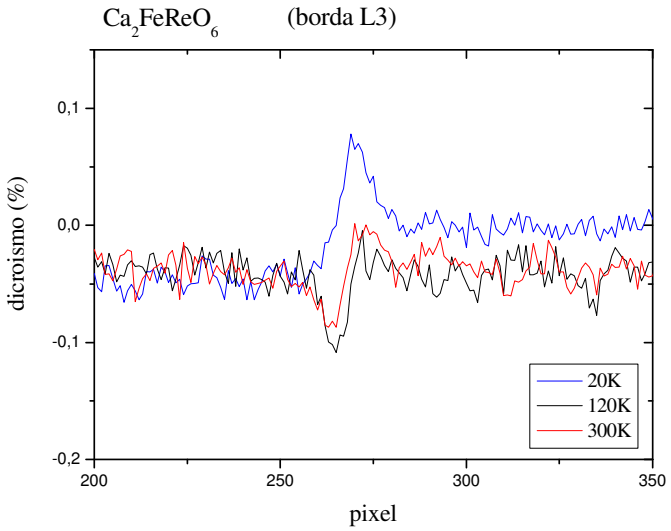

Gráfico3. Sinal de dicroismo em percentagem em função de pixel para a borda L_3 do Re, que está em uma faixa de energia em torno de 10.500eV

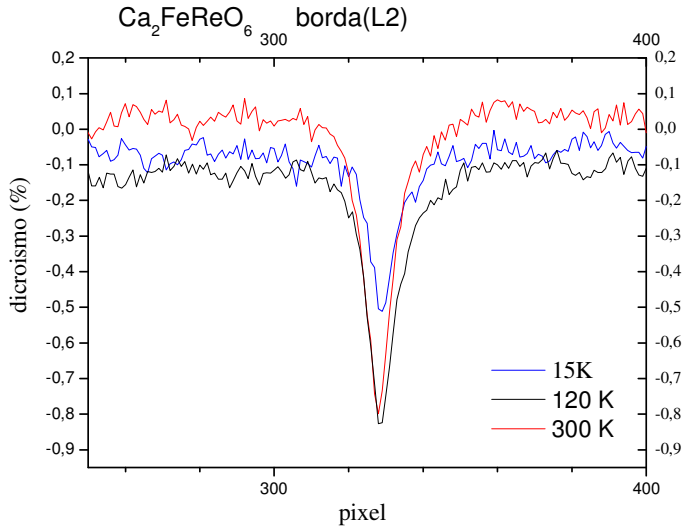

Gráfico 4. Sinal de dicroismo em percentagem função de pixel para a borda L_2 do Re que se encontra em uma energia de aproximadamente 11.900eV.

Análise dos dados

Analisando o gráfico 1 pudemos verificar a existência de uma transição de fase em torno de 150K, fato que já havia sido comprovado por estudos anteriores [i], sendo assim abaixo desta temperatura não esperávamos nenhuma mudança na estrutura eletrônica do composto e em consequência, nenhuma variação muito grande no sinal de dicroísmo abaixo dessa temperatura.

O gráfico 2 nos mostra as curva de magnetização para 15K e 300K. Como podemos ver, a saturação da curva ocorre para campos altos, pois o campo coercitivo existente na amostra é muito alto e dependente da temperatura. Sendo assim, para baixos campos a magnetização para um dado campo é muito sensível à temperatura. Este fato implica que, para o campo de 725 G aplicado à amostra nas medidas de dicroísmo, não magnetizamos completamente a amostra, sendo diferente a magnetização a diferentes temperaturas aplicadas. Como análises quantitativas a partir de medidas de dicroísmo devem ser feitas em condição de saturação magnética, não foi possível quantificar o momento magnético do Re.

A partir dos gráficos 3 e 4 percebemos que existe um sinal de dicroísmo, muito mais forte na boda L_2 do que na borda L_3 do Re, porém ambos confirmam de uma maneira definitiva a antes discutida existência de um momento magnético do Re. Como podemos ver, há uma variação do sinal de dicroísmo entre temperaturas próximas de 20K e 120K, sendo muito parecidas o sinal de dicroísmo entre 120K e 300K, esta também é uma forte evidencia de mudanças na estrutura eletrônica do composto e na natureza magnética do Re, como já havíamos discutido anteriormente. Um estudo detalhado do sinal de dicroísmo em função da temperatura mostrou que essas mudanças ocorrem de fato em um intervalo restrito de temperaturas em torno de 120 K, sugerindo de fato uma transição de fase com participação dos íons de Re, em uma temperatura próxima à esperada pelas medidas anteriores de difração de nêutrons[i] .

Conclusão

A partir dos estudos realizados sobre a amostra Ca_2FeReO_6 e sobre a linha de luz DXAS conseguiu-se demonstrar a existência de momento magnético do Re e uma transição de fase em torno de 120 K.

A quantificação do momento magnético do Re não foi possível devido ao fato do campo coercitivo da amostra ser muito grande em relação ao campo aplicado, porém iremos realizar novas medidas com campos da ordem de 9000 G capaz de magnetizar completamente o material. Este eletroímã já está disponível no Laboratório Nacional de Luz Síncrotron, e este estudo será de fato realizado no futuro, com o objetivo de quantificar este momento e estudar mais profundamente a transição de fase existente neste material.

Descobrimos que a física relacionada a este composto é realmente muito interessante como sugerido pelas medidas iniciais de difração de nêutrons, o que nos motivou a escrever um projeto de tese de doutorado que tem como título “Sondando os Graus de Liberdade de Spin e Orbital em Óxidos de Metais de Transição através de Interações dos Raios-X com a Matéria” e que será realizado com a orientação do Prof.

Dr. Eduardo Granado. Será aprofundado o estudo dessas mudanças elétrônicas e magnéticas futuramente utilizando como uma das ferramentas também programas de simulação para sinais de absorção e dicroísmo de raios-x em função de parâmetros como campo cristalino, acoplamento de Hund, distâncias interatômicas, etc.

Referências

[i] E. Granado, Q. Huang, J. W. Lynn, J. Gopalakrishnan, R. L. Greene and K.Ramesha, Phys.Rev. B **66**, 064409 (2002).

[ii] J. C. Cezar, Estudo de propriedades magnéticas em materiais granulares por espectroscopia de absorção de raios X, Universidade Estadual de Campinas Instituto de Física Glab Wataghin (2003).

[iii] H. Karo, T. Okuda, Y. Tomioka, K. Oikawa, T. Kamiyama and Y. Tokura, Phys.Rev. B **65**, 144404 (2002)

[iv] S. W. Lovesey and S.P. Collins, X-Ray Scattering and Absorption by Magnetc Materials, Oxford series on Syncrotron Radiation (1996).

Spin-orbital ordering and mesoscopic phase separation in the double perovskite Ca_2FeReO_6

E. Granado,[1,2,*] Q. Huang,[1,3] J. W. Lynn,[1,2] J. Gopalakrishnan,[2,4] R. L. Greene,[2] and K. Ramesha[4]
[1]*NIST Center for Neutron Research, National Institute of Standards and Technology, Gaithersburg, Maryland 20899*
[2]*Center for Superconductivity Research, University of Maryland, College Park, Maryland 20742*
[3]*Materials Engineering Program, University of Maryland, College Park, Maryland 20742*
[4]*Solid State and Structural Chemistry Unit, Indian Institute of Science, Bangalore 560012, India*
(Received 1 April 2002; revised manuscript received 7 May 2002; published 6 August 2002)

Neutron powder diffraction measurements on Ca_2FeReO_6 reveal that this double perovskite orders ferrimagnetically and shows anomalous lattice parameter behavior below $T_C = 521$ K. Below ~ 300 K and ~ 160 K we observe that the high-T monoclinic crystal structure separates into two and three monoclinic phases, respectively. A magnetic field suppresses the additional phases at low T in favor of the highest-T phase. These manifestations of the orbital degree of freedom of Re $5d$ electrons indicate that these electrons are strongly correlated and the title compound is a Mott insulator, with competing spin-orbitally ordered states.

DOI: 10.1103/PhysRevB.66.064409 PACS number(s): 75.30.Gw, 61.12.Ld, 64.75.+g, 75.25.+z

I. INTRODUCTION

Novel phenomena caused by electrons localized in degenerate orbital states have been the central issue in the physics of transition-metal oxides for the last few years. For e_g orbital systems, the degeneracy under cubic crystalline fields is often removed by large Jahn-Teller distortions of the oxygen octahedra. The physics of electrons localized in partly occupied t_{2g} orbitals is quite different, due to the relative weakness of the Jahn-Teller coupling, higher degeneracy, and additional symmetry of t_{2g} orbitals. In addition, these electrons may show unquenched orbital magnetic moments, and spin-orbit coupling usually plays an important role.

The double-perovskite compounds $A_2Fe(Mo,Re)O_6$ (A = Ca, Sr, or Ba) have recently attracted much scientific and technological interest after the discovery of large tunneling magnetoresistance at room temperature in most cases,[1–6] which has been ascribed to half-metallic electronic band structures.[1,2,7–11] An intriguing exception is the insulating behavior found in the compound Ca_2FeReO_6 (CFRO),[3] revealing that the (Fe,Re)-based double perovskites are at the border of a metal-insulator transition.[4] Mössbauer studies in CFRO indicate the presence of Fe^{3+} ions;[4] thus the oxidation state of Re ions is expected to be $5+$, with two electrons in the $5d$ t_{2g} orbitals. In order to search for possible manifestations of the Re t_{2g} orbital degree of freedom[12] in this insulating compound, the nuclear and magnetic structures were investigated by neutron powder diffraction. A number of remarkable observations were made, to be described in this paper: (i) mesoscopic phase separations, with coexisting monoclinic crystal structures below ~ 300 K and large changes in the phase proportions below $T_s \sim 160$ K; (ii) magnetic-field (H) control of the volume fractions in the phase-separated state at 100 K, with a suppression of the additional phases observed below ~ 300 K for an applied field of a few tesla; (iii) a ferrimagnetic arrangement of Fe and Re magnetic moments below $T_C = 521$ K, with strong evidence for distinct moment directions for the competing phases; (iv) anomalous lattice parameter behavior below T_C; and (v) a new Bragg peak below T_s, which is forbidden by the symmetry considered to model the nuclear structure. These results indicate that the Re^{5+} t_{2g}^2 electrons are localized on an atomic scale and CFRO is a Mott insulator. The mesoscopic phase separations observed for this compound are ascribed to a competition between distinct spin and orbitally ordered insulating states.

II. EXPERIMENTAL DETAILS

The preparation procedures and characterization of the ceramic pellets of CFRO used in this work are described in Refs. 3 and 4. The high-resolution neutron powder diffraction measurements were performed on the BT-1 powder diffractometer at NIST Center for Neutron Research, using monochromatic beams with $\lambda = 1.5402(1)$ Å, 1.5903(1) Å, and 2.0783(1) Å, produced by Cu(311), Si(531), and Ge(311) monochromators, respectively. Typical collimations were 15′, 20′, and 7′ arc before and after the monochromator, and before detectors, respectively. The intensities were measured in steps of 0.05° in the 2θ range 3°–168°. Data were collected at various temperatures in the range 10–650 K. Crystal and magnetic structure refinements were carried out using the program GSAS.[13] The nuclear scattering amplitudes are 0.490, 0.954, 0.920, and 0.581 ($\times 10^{-14}$ m) for Ca, Fe, Re, and O, respectively.[13] T-dependent measurements were performed on warming the sample.

III. RESULTS AND ANALYSIS

Above ~ 520 K, we found that this compound is nonmagnetic and exhibits monoclinic structure with $P2_1/n$ symmetry and the unit cell size $\approx \sqrt{2}a_p \times \sqrt{2}a_p \times 2a_p$ and $\beta \approx 90°$,[14] where a_p is the unit-cell size of the primitive perovskite. Initial structural parameters used in the refinement were taken from Ref. 4. A minor Fe_3O_4 impurity (0.6% weight fraction) was identified. Due to the small phase fraction of this impurity phase, a simplified cubic spinel unit cell (space group $Fd3m$) was used in the refinements at all T, despite the well-known Verwey transition to a monoclinic superstructure below ~ 120 K.[15–19] Concerning the main phase, the refined occupancies are 0.93(2), 0.96(2), 1, and 0.98(2)

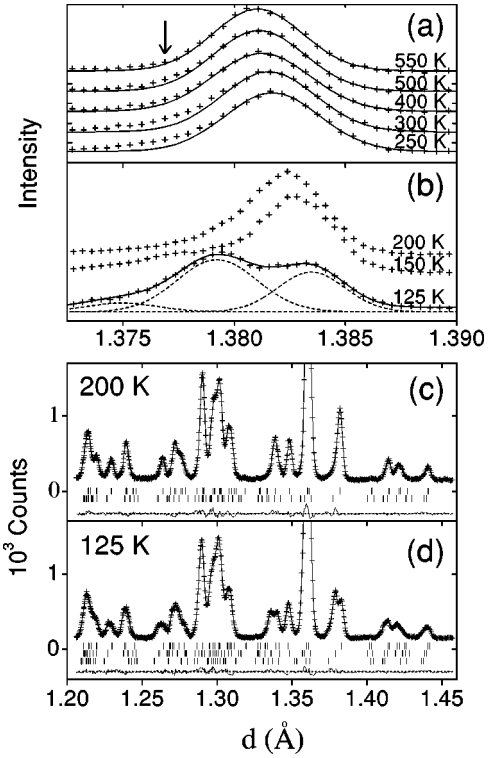

FIG. 1. (a),(b) Crosses: *T*-dependence of the neutron powder diffraction of Ca_2FeReO_6 around the (040) Bragg reflection, at $250K \leqslant T \leqslant 550$ K (a) and $125\,\mathrm{K} \leqslant T \leqslant 200$ K (b). The solid lines in (a) are Gaussian curves. The lines in (b) illustrate a three-Gaussian fit for the scattering at $T = 125$ K. (c),(d) Crosses: selected portion of the neutron powder profile of Ca_2FeReO_6 at $T = 200$ K (c) and $T = 125$ K (d). The solid lines indicate the calculated profiles using two (c) and three (d) distinct monoclinic phases as the structural model (see text). The differences between experimental and calculated profiles are given as solid lines in the bottom of the figures. Short vertical lines correspond to Bragg peak positions for M1 and M2 (c) and M1, M2, and SP (d).

for Ca, Fe, Re, and O, respectively. Quoted errors in this manuscript are statistical and represent one standard deviation. Due to the similar neutron scattering lengths of Fe and Re, the degree of Fe and Re ionic ordering in our sample was not estimated by neutron diffraction. Previous x-ray diffraction studies[2,4] indicated that the Fe/Re double-perovskite system has a strong tendency for ionic ordering ($\sim$95% for our sample[4]).

Phase separations were observed for CFRO. Figure 1(a) shows the (040) nuclear reflection for $250\,\mathrm{K} \leqslant T \leqslant 550$ K. Gaussian solid lines fitting the higher-*d*-spacing side of the peak are also displayed. At 550 K, the good fit indicates a single peak, within our resolution. Below $\sim$500 K, however, a residual intensity which increases with decreasing *T* is observed on the lower-*d*-spacing side, suggesting the presence of a second peak. Below $\sim$300 K, we were able to obtain stable refinements including a second monoclinic phase in the model, which improved significantly the overall fit to the observed intensities. This phase is referred to as M2.[20] As shown in Fig. 1(b), the intensity on the lower-*d*-spacing side of the (040) reflection increases sharply, and this reflection

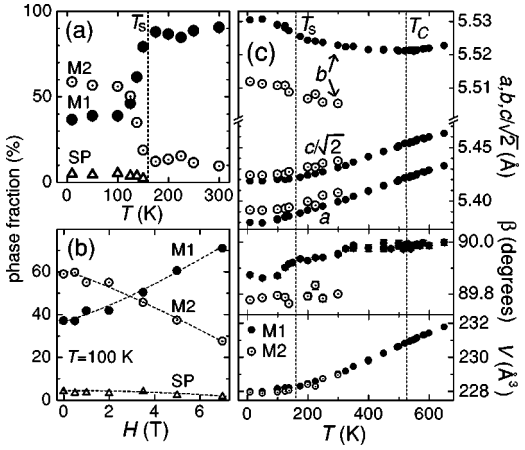

FIG. 2. (a) *T* dependence of the relative fractions of coexisting phases M1, M2, and SP for Ca_2FeReO_6. (b) Magnetic-field dependence of the relative fractions of M1, M2, and SP at 100 K. The dashed lines are guides to the eyes. (c) *T* dependence of the lattice parameters *a*, *b*, and *c*, monoclinic angle β, and unit cell volume *V* of M1 (solid circles), and M2 (open circles). Error bars are smaller than the symbol sizes.

becomes three peaks below $T_s \sim 160$ K. A three-Gaussian fit at 125 K is illustrated (lines). In the final refinements below T_s, excellent fits were obtained by using three monoclinic phases (M1, M2, and SP), with slightly different lattice parameters. At 540 K, in the single-phase regime (besides the Fe_3O_4 impurity phase), the coefficients describing the Bragg peak linewidths indicate a lattice strain of 0.22(1)% full width at half maximum (FWHM) for CFRO. Below 300 K, where phase separations were clearly observed, such coefficients had to be constrained to be the same for the coexisting CFRO phases, in order to avoid large correlations between the fitting parameters. Under this constraint, an average lattice strain of 0.35(2)% FWHM was inferred for the coexisting CFRO phases at 100 K, larger than the strain for the single CFRO phase at 540 K. No particle size broadening was observed at 100 K, within our resolution, indicating that the M1 and M2 domains are larger than $\sim$1000 Å. Figures 1(c) and 1(d) show a portion of the observed and calculated intensities for models with two phases (200 K) and three phases (125 K), respectively.

Figure 2(a) shows the M1, M2, and SP phase fractions in the *T* interval in which multiphase Rietveld refinements were performed ($\leqslant$300 K). Above 300 K, a small fraction of M2 ($\leqslant$5%) may be still present [see Fig. 1(a)]. The M2 fraction remains nearly constant at $\sim$12% between $\sim$300 K and T_s, rapidly develops to $\sim$55% below T_s, and then remains constant again below $\sim$100 K. The SP fraction develops up to $\sim$5% below T_s.

Figure 2(b) shows the *H* dependence of the M1, M2, and SP fractions. The magnetic field was applied using a superconducting vertical-field magnet after zero-field (ZF) cooling the sample to 78 K, followed by a ZF warming to 100 K. The profiles were analyzed under the same structural model described above. Only high-angle data with negligible magnetic contributions were used in the refinement of the nuclear structure under applied *H*. The magnetic field suppresses the

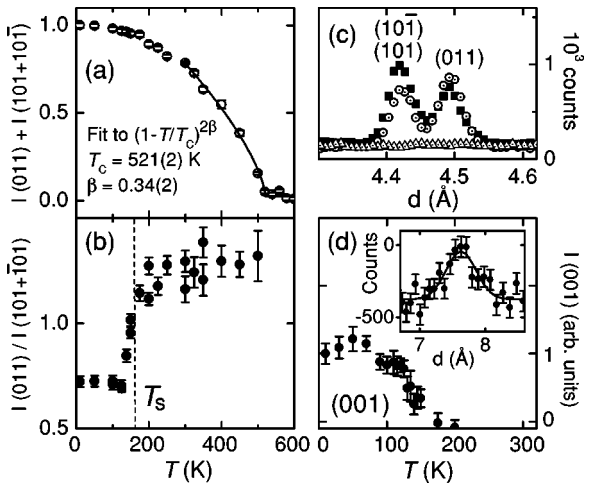

FIG. 3. (a) T dependence of the sum of intensities of the (011), (101), and $(10\bar{1})$ Bragg peaks for Ca_2FeReO_6, normalized at 10 K. The solid line is a fit to a power law, giving $T_C = 521(2)$ K, and a critical exponent $\beta = 0.34(2)$. (b) T dependence of the ratio of the intensity of the (011) reflection and the sum of the (101) and $(10\bar{1})$ (unresolved) Bragg reflections. (c) The data at $T = 100$ K (solid squares), $T = 200$ K (open circles), and $T = 550$ K (open triangles). (d) T dependence of the intensity of the peak at the (001) position. The inset shows the data at 10 K, subtracted from 300 K, and a Gaussian fit.

M2 fraction, from 55% to 22%, as the field increases to 7 T. The original phase fractions are fully restored after the release of H.

Magnetic intensities superposed on the nuclear Bragg peaks were observed at low angles below ~ 520 K. Figure 3(a) shows the sum of the integrated intensities of the (011), (101), and $(10\bar{1})$ reflections as a function of T, indicating that the magnetic ordering occurs below 521 K (T_C), in reasonable agreement with $T_C \sim 540$ K obtained by magnetization measurements.[21,22] Above T_s, a ferrimagnetic model for the Fe and Re moments (M_{Fe} and M_{Re}, respectively) lying in the ac plane gives a good fit to the observed data. The angle between the moments and the a axis is $\varphi = 55(2)°$, obtained at 400 K, and remains constant within two standard errors for $T_s < T < T_C$. As shown in Fig. 3(b), the ratio of the (011) and $(101)+(10\bar{1})$ intensities remains constant above T_s, agreeing with the conclusion that the spin direction does not change in this T range. Below T_s, this ratio decreased sharply [see also Fig. 3(c)], indicating a change in the average spin structure, and then remained constant below ~ 100 K. This behavior is clearly related to the phase separation. The constant moment direction ($\hat{\mathbf{m}}$) above T_s allows us to assume that $\hat{\mathbf{m}}(\mathrm{M1})$ does not change with T. We then modeled the magnetic structure below T_s, keeping $\hat{\mathbf{m}}(\mathrm{M1})$ fixed and allowing $\hat{\mathbf{m}}(\mathrm{M2}) \neq \hat{\mathbf{m}}(\mathrm{M1})$, and found that $\hat{\mathbf{m}}(\mathrm{M2})$ is nearly parallel ($\pm 5°$) to the b axis. The sharp changes in the relative intensities of the magnetic peaks between 100 K and T_s are due to the changes of the M1 and M2 phase proportions [see Fig. 2(a)]. The moments were constrained to be the same for M1, M2, and SP in the final refinements, yielding $M_{Fe} = 3.42(7)\mu_B$ and $M_{Re} = 1.02(7)\mu_B$ at 10 K, pointing in opposite directions. These values agree reasonably well with $(3.76–4.29)\mu_B$ and $(1.07–1.33)\mu_B$ for Fe and Re, respectively, predicted by band structure calculations for this compound.[9]

The T dependence of the lattice parameters for M1 and M2 is shown in Fig. 2(c). For M1, the a and c axes decrease smoothly as T decreases, while the b axis shows a negative thermal expansion for $T \lesssim 520\,\mathrm{K} \approx T_C$, crossing over to conventional behavior above T_C. This effect was not observed in the metallic isostructural compound Ca_2FeMoO_6.[23,24] According to our refinements, the monoclinic angle $\beta(M1)$ is very close to 90° above ~ 300 K and shows inflection points at ~ 300 K and T_s. This result suggests that the crystal structure of M1 is distorted by the phase separation. The unit-cell volume decreases smoothly for decreasing T and does not indicate any metal-insulator transition for this compound. Compared to M1, M2 has shorter b, longer a and c, smaller β, and slightly smaller V. The application of a magnetic field $H \leqslant 7$ T at 100 K is responsible for a slight ($\lesssim 0.01$ Å) decrease of the b axes, increase of the a and c axes, and no significant changes in β and V for both M1 and M2.

The average bond distances between the transition metal (M) and oxygen ions in the MO_6 octahedra are 2.02 Å and 1.95 Å at room temperature for the two independent crystallographic M sites in the $P2_1/n$ symmetry. Based on considerations of the ionic radius, the bond distance of 2.02 Å would favor either Fe^{3+} or Re^{4+} ions, and that of 1.95 Å would favor either Re^{5+} or Fe^{4+}; because the neutron scattering lengths of Fe and Re are similar, we cannot identify the M sites directly from the refinement. Since a Mössbauer spectrum on this sample[4] is consistent with Fe^{3+}, we conclude that the largest M ion corresponds to Fe^{3+}, while the smallest M ion is Re^{5+}. The differences of Fe-O distances are very small [from 2.010(4) Å to 2.033(3) Å], as well as of Re-O distances [from 1.945(4) Å to 1.954(3) Å]. Also, the O-M-O angles are very close to 90° ($\pm 1°$), indicating a very small distortion for the MO_6 octahedra. Bond-valence calculations[25] using the refined Fe-O distances give a valence of $+2.94$ for Fe. The changes in the M-O bond distances with T and between M1 and M2 are very small, within three standard errors, showing that M1 and M2 cannot be easily discerned on the basis of the Fe and Re oxidation states. No anomalous changes in the bond distances caused by the phase separation could be observed in our experiment.

In order to search for weak Bragg reflections, complementary measurements were taken on the BT-2 triple-axis spectrometer at NIST with $\lambda = 2.359$ Å and relaxed collimations, providing much stronger signal than the high-resolution measurements. The inset of Fig. 3(d) shows the energy-integrated neutron scattering at high d spacings, at 10 K subtracted from 300 K. We observed a weak peak at $d = 7.62(3)$ Å close to the (001) position for CFRO. The integrated intensity is as weak as $\sim 0.1\%$ of the strongest nuclear Bragg peak, 1.2(2)% of the sum of the $(011)+(101)+(10\bar{1})$ magnetic intensities at 10 K, and $\sim 5\%$ of the principal Bragg peaks of the Fe_3O_4 impurity phase. An attempt to determine the nuclear or magnetic nature of this peak di-

rectly by polarization analysis was unsuccessful, since the neutron beam was depolarized by the sample. This peak likely originates from M2, given the clear correlation of its intensity with the M2 phase fraction [see Figs. 2(a) and 3(d)]. On the other hand, the crystal structure of the Fe_3O_4 impurity phase is distorted from cubic symmetry with cell parameter a^* to a monoclinic $\sqrt{2}a^* \times \sqrt{2}a^* \times 2a^*$ supercell with Cc space group symmetry below ~ 120 K.[15–19] Thus, (1,0,1/2) and (0,1,1/2) superstructure Bragg peaks (cubic notation) from Fe_3O_4 might be expected below 120 K, at $d = 7.504(3)$ Å using the refined a^* for our impurity phase or at $d = 7.514\,44(3)$ Å and $d = 7.496\,97(3)$ Å using the extended monoclinic cell and lattice parameters reported in Ref. 19. However, the differences between the d spacing for the forbidden Bragg peak observed for CFRO and the expected positions for the superstructure reflections for Fe_3O_4 are statistically significant (about four standard deviations). Second, the intensities of the strongest Fe_3O_4 superlattice peaks are typically $\lesssim 1\%$ of those of the principal peaks.[19] Since Fe_3O_4 superlattice peaks with wave vectors (1,0,1/2) and (0,1,1/2) were found to be particularly weak,[18] these reflections are expected to much weaker than the observed peak at $d = 7.62(3)$ Å and low T for our sample. We also note that significant intensities were observed for this peak between 120 K and 150 K, therefore above the Verwey transition for Fe_3O_4. We conclude that this peak cannot be ascribed to the impurity phase and it is due to CFRO. There are thus two possible origins of this peak: (i) a nuclear reflection related to a symmetry reduction, since this peak is forbidden by $P2_1/n$ symmetry. However, we were not able to model a lower symmetry to refine the structure of either M1 or M2, since the intensities of the peak at (001) position and any other forbidden reflections are too weak to be detected in high-resolution measurements. (ii) An antiferromagnetic canting in the Re and/or Fe magnetic sublattices, with the propagation vector along one particular Fe-Re-Fe binding direction.

In order to search for spin excitations in CFRO at room temperature, inelastic neutron scattering measurements were performed close to the (000) reciprocal lattice point, using the BT-9 triple-axis spectrometer at NIST. Details of the method are given in Ref. 26. The incident energy was chosen to be 13.5 meV, and collimations of 10′-10′-10′-10′ FWHM were used. No excitations were detected within our experimental range. We note that the accessible window in energy-momentum space is very limited around the (000) Bragg point, and the nonobservation of spin excitations is indicative of a gap larger than ~ 0.5 meV in the spin-wave dispertion or, alternatively, a spin stiffness constant larger than ~ 200 meV Å^2 at room temperature.

IV. DISCUSSION

The anomalous expansion of the b-lattice parameter for decreasing T below T_C [see Fig. 2(c)] clearly suggests a simultaneous spin and orbital-ordering transition, which can be ascribed to a significant spin-orbit coupling of t_{2g} electrons with unquenched orbital magnetic moments. We attribute this to the Re^{5+} orbital degree of freedom, since high-spin Fe^{3+} ions are not orbitally active.

Phase separations occur in our CFRO sample below room temperature, indicating a close competition between distinct physical states with similar free energies over a large T interval. The delicate energetic balance between these states is demonstrated by the decisive influence of a magnetic field of the order of a few tesla on the phase fractions at 100 K. Considering such a close competition, it is clear that even a slight degree of chemical disorder and inhomogeneity may stabilize the phase-separated state against a more conventional first-order transition at a definite temperature. Below ~ 160 K (T_s), three coexisting phases were detected (M1, M2, and SP). The SP fraction is small at all T and may be a strain phase which underlies the coexistence of M1 and M2. Concerning the main phases, their fractions being tuned by an applied magnetic field at 100 K shows that M1 and M2 have distinct magnetic structures. A simple collinear ferrimagnetic model was sufficient to obtain a satisfactory refinement of our high-resolution data below T_C, with different moment orientations for M1 and M2 below T_s. On the other hand, high-intensity measurements reveal a weak peak below T_s at the (001) position, which intensity correlates with the M2 fraction, indicating a noncollinear magnetic structure or, alternatively, a symmetry reduction for M2. Both possibilities suggest that M2 represents an orbitally ordered pattern of the Re^{5+} t_{2g} electrons which is distinct from the orbitally ordered structure of M1.

Extensive research has shown that mesoscopic phase separation plays a key role in the colossal magnetoresistance effect observed for a number of manganite compounds, where insulating and metallic coexisting phases may be tuned by applied magnetic fields.[27] Although CFRO is also close to a metal-insulator transition,[4] the resistivity of this compound shows monotonic insulating behavior below room temperature (Ref. 3); therefore, neither M1 nor M2 seems to be metallic. In fact, our results suggest that the orbital degree of freedom, characteristic of a Mott insulating state, is manifested for both phases, implying that the Re $5d$ electrons are strongly correlated. Recent theoretical investigations in $Sr_2Fe(Re,Mo)O_6$ double-perovskite systems support an enhanced effective intra-atomic exchange strength at the Mo or Re site (I_{eff}), due to hybridization with the Fe $3d$ electrons.[7,8] The possibility of a negative effective Coulomb interaction strength $U_{eff} = U - I_{eff}$ due to the enhanced I_{eff} was proposed for Sr_2FeMoO_6.[7] For monoclinic CFRO, the Re t_{2g}–Fe t_{2g} hybridization is reduced due to the significant bending of the Fe-O-Re angle;[9] therefore, smaller values of I_{eff} may be expected. This fact, coupled with the possibly larger U for the Re than for the Mo electrons, may lead to a relatively large U_{eff} for the Re site in CFRO, which may partly account for the Mott insulating state inferred from our experimental data.

ACKNOWLEDGMENTS

We thank A. Santoro, S. Trevino, and D.C. Dender for helpful discussions. This work was supported by NSF-MRSEC, Grant No. DMR 00-80008, U.S., FAPESP, Brazil, and DST, New Delhi, India.

*Present address: Laboratório Nacional de Luz Síncrotron, Caixa Postal 6192, CEP 13083-970, Campinas, SP, Brazil.

[1] K.-I. Kobayashi, T. Kimura, H. Sawada, K. Terakura, and Y. Tokura, Nature (London) **395**, 677 (1998).

[2] K.-I. Kobayashi, T. Kimura, Y. Tomioka, H. Sawada, K. Terakura, and Y. Tokura, Phys. Rev. B **59**, 11 159 (1999).

[3] W. Prellier, V. Smolyaninova, A. Biswas, C. Galley, R.L. Greene, K. Ramesha, and J. Gopalakrishnan, J. Phys. C **12**, 965 (2000).

[4] J. Gopalakrishnan, A. Chattopadhyay, S.B. Ogale, T. Venkatesan, R.L. Greene, A.J. Millis, K. Ramesha, B. Hannoyer, and G. Marest, Phys. Rev. B **62**, 9538 (2000).

[5] A. Maignan, B. Raveau, C. Martin, and M. Hervieu, J. Solid State Chem. **144**, 224 (1999).

[6] J.M. Dai, W.H. Song, S.G. Wang, S.L. Ye, K.Y. Wang, J.J. Du, Y.P. Sun, J. Fang, J.L. Chen, and B.J. Gao, Mater. Sci. Eng., B **83**, 217 (2001).

[7] D.D. Sarma, P. Mahadevan, T. Saha-Dasgupta, S. Ray, and A. Kumar, Phys. Rev. Lett. **85**, 2549 (2000).

[8] Z. Fang, K. Terakura, and J. Kanamori, Phys. Rev. B **63**, 180407(R) (2001).

[9] H. Wu, Phys. Rev. B **64**, 125126 (2001).

[10] A. Chattopadhyay and A.J. Millis, Phys. Rev. B **64**, 024424 (2001).

[11] A.A. Aligia, P. Petrone, J.O. Sofo, and B. Alascio, Phys. Rev. B **64**, 092414 (2001).

[12] Y. Tokura and N. Nagaosa, Science **288**, 462 (2000).

[13] C. Larson and R. B. Von Dreele (unpublished).

[14] For a review of structural aspects of double-perovskite systems, see M.T. Anderson, K.B. Greenwood, G.A. Taylor, and K.R. Poeppelmeier, Prog. Solid State Chem. **22**, 197 (1993).

[15] E.J.W. Verwey, P.W. Haayman, and F.C. Romeijan, J. Chem. Phys. **15**, 181 (1947).

[16] M. Iizumi and G. Shirane, Solid State Commun. **17**, 433 (1975).

[17] J. Yoshido and S. Iida, J. Phys. Soc. Jpn. **47**, 1627 (1979).

[18] M. Iizumi, T.F. Koetzle, G. Shirane, S. Chikazumi, M. Matsui, and S. Todo, Acta Crystallogr., Sect. B: Struct. Crystallogr. Cryst. Chem. **38**, 2121 (1982).

[19] J.P. Wright, J.P. Attfield, and P.G. Radaelli, Phys. Rev. Lett. **87**, 266401 (2001).

[20] For an independent report also showing evidence for phase separation in Ca_2FeReO_6, see W. Westerburg, O. Lang, C. Ritter, C. Felser, W. Tremel, and G. Jakob, Solid State Commun. **122**, 201 (2002).

[21] J. Longo and R. Ward, J. Am. Chem. Soc. **83**, 2816 (1961).

[22] S.E. Lofland, T. Scabarozi, S. Kale, S.M. Bhagat, S.B. Ogale, T. Venkatesan, R.L. Greene, J. Gopalakrishnan, and K. Ramesha, IEEE Trans. Magn. **37**, 2153 (2001).

[23] J.A. Alonso, M.T. Casais, M.J. Martínez-Lope, J.L. Martínez, P. Velasco, A. Muñoz, and M.T. Fernández-Díaz, Chem. Mater. **12**, 161 (2000).

[24] L. Pinsard-Gaudart, R. Surynarayanan, A. Revcolevschi, J. Rodriguez-Carvajal, J-M. Greneche, P.A.I. Smith, R.M. Thomas, R.P. Borges, and J.M.D. Coey, J. Appl. Phys. **87**, 7118 (2000).

[25] I.D. Brown, Acta Crystallogr., Sect. B: Struct. Sci. **48**, 553 (1992).

[26] J.W. Lynn, R.W. Erwin, J.A. Borchers, Q. Huang, A. Santoro, J-L. Peng, and Z.Y. Li, Phys. Rev. Lett. **76**, 4046 (1996).

[27] See E. Dagotto, T. Hotta, and A. Moreo, Phys. Rep. **344**, 1 (2001), and references therein.

Metal-insulator transition of ferromagnetic ordered double perovskites: $(Sr_{1-y}Ca_y)_2FeReO_6$

H. Kato,[1] T. Okuda,[1] Y. Okimoto,[1] Y. Tomioka,[1] K. Oikawa,[2] T. Kamiyama,[2] and Y. Tokura[1,3,4]
[1]*Joint Research Center for Atom Technology (JRCAT), Tsukuba 305-0046, Japan*
[2]*Institute of Materials Structure Science, KEK, Tsukuba 305-0801, Japan*
[3]*Correlated Electron Research Center (CERC), National Institute of Advanced Industrial Science and Technology (AIST), Tsukuba 305-8562, Japan*
[4]*Department of Applied Physics, University of Tokyo, Tokyo 113-8656, Japan*
(Received 26 November 2001; published 15 March 2002)

Temperature- and composition-control metal-insulator (M-I) transitions have been investigated for ordered double perovskites, $(Sr_{1-y}Ca_y)_2FeReO_6$. Ca_2FeReO_6 ($y=1$) shows the thermally induced M-I transition associated with the lattice-structural transition around 150 K. The alloyed system undergoes the M-I transition in the almost fully spin-polarized ground state around $y=0.4$ with minimal enhancement of the electronic specific-heat coefficient but with a large energy-scale (~ 1 eV) change of the optical conductivity spectrum. These results indicate the importance of electron correlation, in particular the orbital correlation of Re t_{2g} electrons, for the ferromagnetic M-I transition.

DOI: 10.1103/PhysRevB.65.144404 PACS number(s): 71.30.+h, 75.40.−s

I. INTRODUCTION

In ordered double perovskites denoted as $A_2B'B''O_6$ (A being an alkaline-earth or rare-earth ion), the transition-metal sites (perovskite B sites) are occupied alternately by different cations B' and B''. Among them, A_2FeMO_6 (A=Ca, Sr, Ba; M=Mo, Re) are known to form conducting ferromagnets, in which Fe^{3+} ($3d^5, S=5/2$) and Mo^{5+} ($4d^1, S=1/2$) [or Re^{5+} ($5d^2, S=1$)] couple antiferromagnetically. Pioneering studies of these materials were done in the 1960s.[1–3] More lately, it was shown by the first-principles band calculation[4,5] that the conduction band around the Fermi energy in Sr_2FeMoO_6 (Sr_2FeReO_6) is occupied solely by the Mo^{5+} $4d$ ($Re^{5+}5d$) t_{2g} down-spin electrons hybridized with the Fe^{3+} $3d$ t_{2g} down-spin state, leading to a half-metallic (single-spin) character. It has also been demonstrated[4–6] that the polycrystalline ceramics of these oxides show a large, low-field magnetoresistance even at room temperature that can be ascribed to the tunneling-type magnetoresistance occurring at the grain boundaries. The phenomena must reflect the high-spin polarization of conduction electrons characteristic of the half-metal as well as the inherently high magnetic transition temperature (T_c) in the range of 400–450 K.[1,2] Thus, the family of half-metallic double perovskites has been attracting growing interest also in light of potential spin-electronic materials.

Among this family, Ba_2FeReO_6,[3] Ba_2FeMoO_6,[7] and Ca_2FeMoO_6 (Ref. 8) show ferromagnetic and metallic characteristics as do Sr_2FeMoO_6 and Sr_2FeReO_6. On the other hand, Ca_2FeReO_6 is rather unique: it has been known to be a ferromagnetic but also an insulating oxide with very high $T_c=538$ K.[9] The crystal symmetry is known as monoclinic,[10] which does not differ from that of metallic Ca_2FeMoO_6.[8] The Fe-O-Mo and Fe-O-Re angles in those Ca-based compounds with a relatively small tolerance factor are also comparable, about 152° and 156°, respectively,[8,10] although the respective angles are appreciably smaller than in the Sr-based analogs, Sr_2FeMoO_6 and Sr_2FeReO_6, with a nearly straight Fe-O-Mo(Re) bond. It is well known for perovskites of transition-metal oxides[11] that such a bond-angle distortion reduces the effective d-electron hopping (supertransfer) energy or the one-electron bandwidth via the reduced hybridization between transition-metal d and oxygen p states. In fact, the variation of the bond angle with the change of A-site ionic size occasionally causes drastic electronic changes,[11] such as the bandwidth-control Mott transition and the colossal magnetoresistance. Thus, the lattice effect induced by Ca substitution as well as the change in electronic configuration between Mo and Re appears to be responsible for the metal-insulator (M-I) phenomena in the family of the ordered double perovskites.

In this paper, we investigate magnetic, electronic, thermal, and structural properties for the A-site solid solutions of ordered double perovskites, $(Sr_{1-y}Ca_y)_2FeReO_6$, to reveal composition-controlled as well as thermally induced M-I transitions. The M-I transition at the ground state may occur via the change of the bandwidth, while keeping the full spin polarization of the conduction electrons; that is, from a half-metal to a ferromagnetic (or ferrimagnetic) insulator with full moment, where the orbital degree of freedom should play an important role in the M-I transition as the only relevant degree of freedom.[12] This class of the M-I transition is intriguing, though, to our best knowledge, it has never been investigated in detail, also from the viewpoint of spin-electronic functionality.

II. EXPERIMENT

Polycrystalline samples of $(Sr_{1-y}Ca_y)_2FeReO_6$ ($0 \leqslant y \leqslant 1$) were prepared by solid-state reaction. The mixture of SrO, CaO, Fe_2O_3, Re_2O_7, and Re was weighted to a prescribed molar ratio and fired at 1173 K for 3 h in evacuated sealed silica tubes. Then, the samples were pelletized, and sintered at 1373 K for 3 h in evacuated sealed silica tubes. The composition of synthesized polycrystals was confirmed to be stoichiometric (Sr:Ca:Fe:Re=$2-2y$:$2y$:1:1) by induction coupled plasma spectroscopy analysis. The crystal

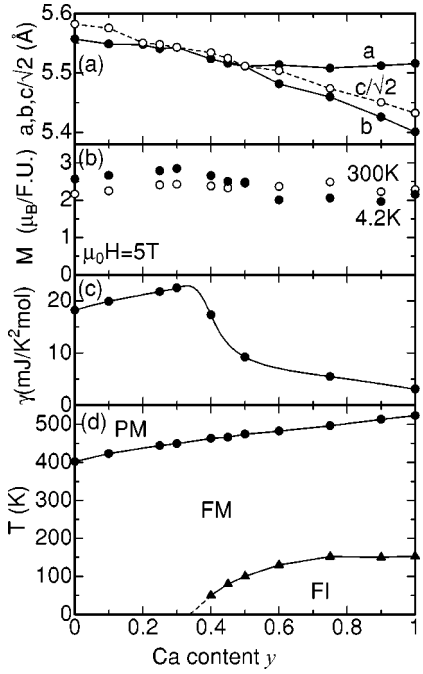

FIG. 1. The y dependence of (a) lattice constants, (b) magnetization (M) at a field of 5 T, (c) the electronic specific-heat coefficient γ, and (d) the electronic phase diagram of $(Sr_{1-y}Ca_y)_2FeReO_6$. PM, FM, and FI in (c) stands for paramagnetic metal, ferromagnetic metal, and ferromagnetic (or ferrimagnetic) insulator, respectively. Solid lines and dashed lines are merely guides to the eyes.

structure was checked by powder x-ray diffraction. The crystal symmetry at room temperature was tetragonal $I4/mmm$ ($y<0.5$) and orthorhombic $Pmm2$ ($y>0.5$). Figure 1(a) shows the lattice constants of $(Sr_{1-y}Ca_y)_2FeReO_6$. At $0.3<y<0.5$, the length of $c_0/\sqrt{2}$ is almost the same as that of a_0, indicating nearly cubic symmetry. The Rietveld refinement also indicated that the degree of ordering of Fe and Re on the B sites was more than 95% in all the samples. As for the end ($y=1$) compound Ca_2FeReO_6, neutron powder-diffraction data were also collected at various temperatures to obtain the precise structural properties.[13]

Magnetization was measured with a commercial superconducting quantum interference device magnetometer. The ac susceptibility up to 550 K was also measured to evaluate the ferromagnetic transition temperature T_c by a resistance bridge. Resistivity was measured with a standard dc four-probe technique. The specific heat was measured by the relaxation method down to 0.5 K. We measured reflectivity spectra $[R(\omega)]$ for $(Sr_{1-y}Ca_y)_2FeReO_6$. $R(\omega)$ spectra were measured using a Fourier-transform-type interferometer for 0.01–0.8 eV and a grating-type monochromator for 0.6–36 eV. For the measurement above 5 eV, we made use of synchrotron radiation at the Ultraviolet Synchrotron Orbital Radiation Facility, Institute for Molecular Science. The temperature (T) dependence of the spectra was measured from 0.01 to 3.0 eV and extrapolated by the room-temperature data above 3 eV. The optical conductivity spectra $[\sigma(\omega)]$ were obtained by a Kramers-Kronig analysis of $R(\omega)$.

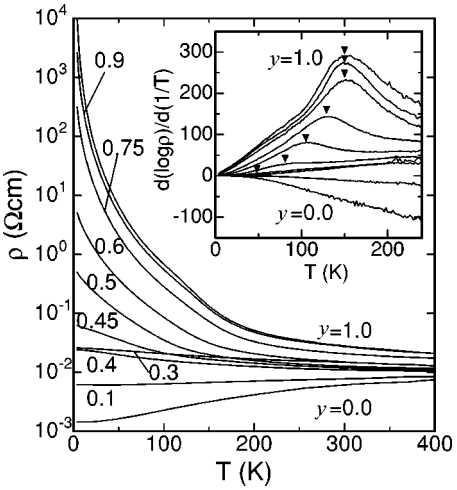

FIG. 2. The temperature (T) profiles of resistivity (ρ) of $(Sr_{1-y}Ca_y)_2FeReO_6$ ($0\leq y\leq 1$). The inset shows the T dependence of $d(\log_{10}\rho)/d(1/T)$.

III. RESULTS AND DISCUSSION

A. Phase diagram of $(Sr_{1-y}Ca_y)_2FeReO_6$

Figure 2 shows the T dependence of resistivity (ρ) for $(Sr_{1-y}Ca_y)_2FeReO_6$. While ρ is about 10^{-2} Ω cm at room temperature for all the samples, the Ca content (y) affects the T dependence of ρ dramatically. For $y\leq 0.3$ the compounds show a metallic or semimetallic behavior down to the lowest temperature. For $y\geq 0.4$, ρ increases with decreasing temperature below 150 K. The variation of the T dependence of ρ with y is more clearly discerned in $d(\log_{10}\rho)/d(1/T)$-T curves as shown in the inset to Fig. 2. For $y\leq 0.3$ the curves show no anomaly, but for $y\geq 0.4$ they have peaks at 100–150 K, indicating an electronic change around this peak temperature (T^*).

Figure 1(d) shows the electronic phase diagram of $(Sr_{1-y}Ca_y)_2FeReO_6$. Although $d\rho/dT<0$, we assigned the high-T phase above T^* as metallic, based on the relatively high conductivity as well as the spectral shape of $\sigma(\omega)$ that is not gapped (see below). The observed T_c increases monotonically from 400 K to 525 K with increasing y. At room temperature, all the samples are in a ferromagnetic metallic state, while the ferromagnetic insulating state emerges for $y\geq 0.4$ below 150 K. The M-I transition temperature is tentatively defined as the peak temperature of the $d(\log_{10}\rho)/d(1/T)$-T curve that coincides with the structural transition temperature in the case of $y=1$, as shown later. At the compositional phase boundary around $y=0.4$ between the ferromagnetic metallic and the ferromagnetic insulating phases, the coercive force at low temperatures increases and the saturation magnetization decreases, also implying a change in the electronic state. However, the ground-state magnetization is $2.0-2.8\mu_B$/f.u., indicating the almost full spin polarization or moment irrespective of y at the ground state [Fig. 1(b)].

B. Specific heat

The low-temperature specific heat (C) was measured to evaluate the electronic specific-heat coefficient (γ).

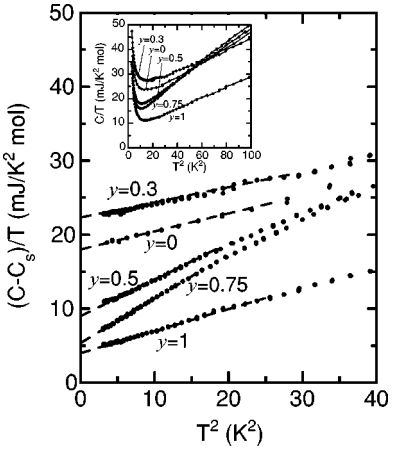

FIG. 3. The low-temperature specific heat of $(Sr_{1-y}Ca_y)_2FeReO_6$ $(0 \leqslant y \leqslant 1)$ plotted as $(C-C_s)/T$ versus T^2. Here, C_s stands for the Schottky component caused by the Re nuclear moments. The inset shows the raw data of specific heat plotted as C/T versus T^2. Dashed lines are merely guides to the eyes.

Figure 3 shows the low-temperature specific heat of $(Sr_{1-y}Ca_y)_2FeReO_6$ plotted as $(C-C_s)/T$ versus T^2. As shown in the inset, the Schottky components (C_s) caused by the Re nuclear moments are dominant at low temperatures (<3 K) in all the compounds that are proportional to $1/T^2$. Coefficients of the $1/T^2$ term are 0.122–0.155 JK/mol, in accord with that reported for Ca_2FeReO_6 $(y=1)$ in a previous work.[9] The value linearly increases with the increase of y, indicating the increase of inner field applied on Re atoms. The γ values were evaluated from the $(C-C_s)/T$ values extrapolated to 0 K at 0 T, because a magnetic field of 6 T was confirmed not to affect the low-temperature specific heat significantly.[14,15] The obtained electronic specific-heat coefficient (γ) is shown in Fig. 1(c). The γ value for $y=0$ is about 18 mJ/K^2 mol, and the density of state at the Fermi level, $N(E_F)$, is estimated to be 4.6×10^{24} $(eV^{-1}\,mol^{-1})$ by using the relation that $\gamma=1/3\pi^2k_B^2N(E_F)$, which is twice as large as the local-density approximation calculation result $[2.1\times10^{24}(eV^{-1}\,mol^{-1})]$.[5] As the M-I phase boundary is approached with the increase of y, the γ value slightly increases and becomes about 22 mJ/K^{2}mol around $y=0.3$. With the increase of y above 0.4, the γ value steeply decreases in accord with the M-I transition, signaling the sudden shrink of the Fermi surface perhaps due to the correlation of the Re t_{2g} orbital as discussed below. Such a behavior is similar to that observed in the filling-control M-I transition in the low-doped region of half-metallic manganites,[15] although γ in the insulating ground state remains finite in the present compound. The increase of the γ value implies the mass-renormalization effect as observed in the vicinity of the Mott transition,[11] but the absence of remarkable enhancement may come from the absence of the spin fluctuation due to the nearly full spin polarization.[15]

C. Optical conductivity

To clarify the electronic-structural change upon the M-I transition for $(Sr_{1-y}Ca_y)_2FeReO_6$, the T and y dependencies

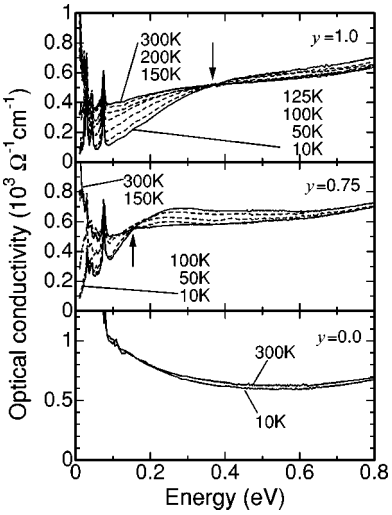

FIG. 4. Optical conductivity spectra of $(Sr_{1-y}Ca_y)_2FeReO_6$ at various temperatures (10–300 K) for $y=0.0$, 0.75, and 1.0.

of the optical conductivity spectrum $\sigma(\omega)$ have been investigated. Figure 4 shows the T dependence of $\sigma(\omega)$ for $y=0$, 0.75, and 1. The spectra are not gapped and contain Drude components below 0.1 eV above 150 K. For $y=0$, $\sigma(\omega)$ above 0.1 eV scarcely changes with the decrease of T down to 10 K. For $y=0.75$ and 1, by contrast, the Drude component disappears and the gap structure appears below 150 K, indicating the occurrence of the M-I transition with the variation of the temperature. The gap formation with the decrease of T accompanies the appreciable change of the optical conductivity spectrum over 1 eV. The spectral weight is transferred from low to high energy through the isosbestic (equal-absorption) point as indicated by vertical arrows in Fig. 4. Such a large-energy-scale change in the course of the M-I transition is characteristic of the Mott transition in the strongly correlated electron system, ensuring that the present half-metallic oxide is also on the verge of the Mott transition.[16] The isosbestic point is observed to gradually decrease with the decrease of y, 0.37 eV and 0.16 eV for $y=1$ and 0.75, respectively. This suggests that the optical gap gradually disappears with the decrease of y toward the ground-state M-I transition point $(y\simeq0.4)$.

D. T dependence of charge dynamics in Ca_2FeReO_6

We summarize in Fig. 5 the T dependence of [Fig. 5(a)] lattice constants, [Fig. 5(b)] spectral-weight loss during the gap formation, [Fig. 5(c)] magnetization, and [Fig. 5(d)] resistivity for Ca_2FeReO_6 $(y=1)$ that shows the typical M-I transition with the variation of T. The low-energy spectral weight of $\sigma(\omega)$ [Fig. 4, upper], that measures the kinetic energy of conduction electrons, is transferred to the high-energy side above the isosbestic point in the course of the M-I transition. To estimate the transferred weight, we have calculated the effective number of electrons $(N_{\rm eff})$, which is defined as

$$N_{\rm eff}(\omega)=\frac{m_0}{\pi e^2 N}\int_0^{\omega_c}\sigma(\omega)d\omega.$$

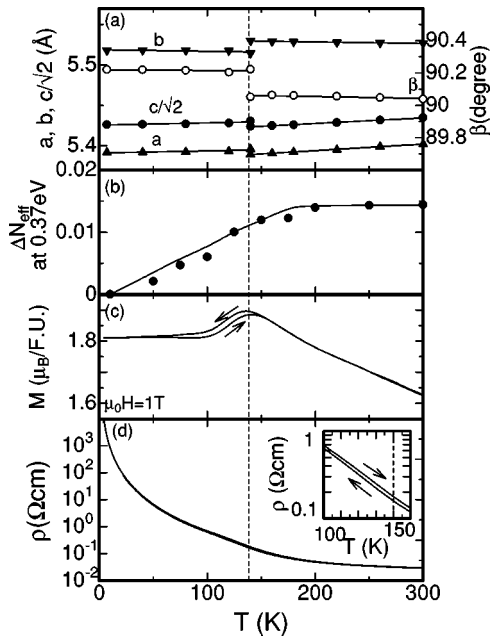

FIG. 5. The temperature (T) dependence of (a) lattice constants, (b) spectral-weight change below 0.37 eV ($\Delta N_{\rm eff}$) due to the charge-gap formation, (c) magnetization (M) at a field of 1 T, and (d) resistivity (ρ) for Ca_2FeReO_6. The inset in (d) shows a magnification of the ρ-T curve at 100–150 K, in which resistivity shows a hysteresis. Solid lines in (a) and (b) are merely guides to the eyes.

Here, m_0 is the free-electron mass and N the number of B-site ion pairs (Fe and Re) per unit volume. The cutoff energy ($\hbar\omega_c$) adopted for the estimate is the isosbestic point, 0.37 eV. The transferred spectral weight $\Delta N_{\rm eff}$ in the course of the M-I transition is represented as $\Delta N_{\rm eff}(T)=N_{\rm eff}(T)-N_{\rm eff}$ ($T=10$ K). Lattice constants were obtained by Rietveld analysis of neutron powder diffraction. As shown in Fig. 5(a), β changes from 90° to 90.2° at 140 K, indicating that the transition from orthorhombic to monoclinic structure takes place. The monoclinic phase is not observed at 160 K, while the nearly orthorhombic phase disappears below 120 K. This means that two phases coexist only in the temperature range of 120–160 K, typical of the first-order transition in the presence of some disorder. The $N_{\rm eff}$ also starts to decrease at 140 K, corresponding to the peak temperature in the $d(\log_{10}\rho)/d(1/T)$ plot. In the corresponding temperature region, thermal hysteresis is observed for magnetization and resistivity, which also reflects the first-order nature of the M-I transition in Ca_2FeReO_6.

It is worth noting that in spite of the existence of the clear optical gap the γ value (T-linear component in specific heat) remains finite even in Ca_2FeReO_6. Note that this cannot be ascribed to the coexistence of the metallic and insulating phases at low temperature, as is evident from the aforementioned neutron-diffraction study on the lattice-structural change. According to the Mössbauer measurements,[10] the valence states of Fe and Re are high-spin Fe^{3+} and Re^{5+}, respectively, and the Re^{5+} $5d\ t_{2g}^2$ states are triply degenerate (or equivalently, a t_{2g} hole can have three degenerate states d_{xy}, d_{yz}, and d_{zx}), retaining the orbital degree of freedom. The correlation of the Re t_{2g} orbital is likely to cause the thermally induced M-I transition, which may be a driving force of the nearly orthorhombic to monoclinic lattice-structural transition as well. Furthermore, Re atoms form an fcc lattice in the ordered double perovskite structure. Then, the nearest-neighboring Re atoms make a tetragon, and hence the orbital ordering of Re^{5+} t_{2g} electrons is likely to be frustrated. The finite γ value in the insulating phase ($y=0.4$–1.0) may be interpreted as the glass state of the Re^{5+} t_{2g} orbital in analogy to the conventional spin-glass state that may give rise to the residual T-linear form of specific heat in spite of the charge-gapped state as observed.

IV. SUMMARY

In summary, we have investigated the M-I phenomena in the ordered double perovskites $(Sr_{1-y}Ca_y)_2FeReO_6$ with controlled one-electron bandwidth. Throughout the composition, the compound is metallic and ferromagnetic at room temperature with high T_c of 400–525 K, but it undergoes the M-I transition with decreasing temperature for $y \geqslant 0.4$. The Ca substitution (y) dramatically affects the electronic structure, and the M-I transition occurs around $y=0.4$ at the ground state while keeping the almost fully spin-polarized state. The ground-state M-I transition, that is not accompanied by appreciable mass renormalization, is likely related to the correlation of the Re t_{2g} orbital. The insulating ground state in the Ca-rich side is perhaps described as the Re t_{2g} orbital ordered state or its glass-state analog associated with the monoclinic lattice distortion.

ACKNOWLEDGMENTS

The authors would like to thank S. Miyasaka, K. Nakanishi, H. Yamada, and N. Nagaosa for enlightening discussions. This work, partly supported by NEDO (New Energy and Industrial Technology Development Organization of Japan), was performed under a joint research agreement between the National Institute of Advanced Industrial Science and Technology (AIST) and the Angstrom Technology Partnership (ATP).

[1] F.K. Patterson, C.W. Moeller, and R. Word, Inorg. Chem. **2**, 196 (1963).

[2] J. Longo and R. Word, J. Am. Chem. Soc. **83**, 2816 (1961).

[3] A.W. Sleight and J.F. Weiher, J. Phys. Chem. Solids **33**, 679 (1972).

[4] K.-I. Kobayashi, T. Kimura, H. Sawada, K. Terakura, and Y. Tokura, Nature (London) **395**, 677 (1998).

[5] K.-I. Kobayashi, T. Kimura, Y. Tomioka, H. Sawada, K. Terakura, and Y. Tokura, Phys. Rev. B **59**, 11 159 (1999).

[6] T.H. Kim, M. Uehara, S-W. Cheong, and S. Lee, Appl. Phys.

Lett. **74**, 1737 (1999).
[7] A. Maignan, B. Raveau, C. Martin, and M. Hervieu, J. Solid State Chem. **144**, 224 (1999).
[8] J.A. Alonso, M.T. Casais, M.J. Martinez-Lope, J.L. Martinez, P. Velasco, A. Munoz, and M.T. Fernanderz-Diaz, Chem. Mater. **12**, 161 (2000).
[9] W. Prellier, V. Smolyaninova, A. Biswas, C. Galley, R.L. Greene, K. Ramesha, and J. Gopalakrishnan, J. Phys.: Condens. Matter **12**, 965 (2000).
[10] J. Gopalakrishnan, A. Chattopadhyay, S.B. Ogale, T. Venkatesan, R.L. Greene, A.J. Millis, K. Ramesha, B. Hannoyer, and G. Marest, Phys. Rev. B **62**, 9538 (2000).
[11] M. Imada, A. Fujimori, and Y. Tokura, Rev. Mod. Phys. **30**, 1039 (1998).
[12] Y. Tokura and N. Nagaosa, Science **288**, 462 (2000).
[13] T. Kamiyama, S. Torii, K. Mori, K. Oikawa, S. Itoh, M. Furusaka, S. Satoh, T. Egami, F. Izumi, and H. Asano, Mater. Sci. Forum **321-324**, 302 (2000).
[14] Y. Tomioka, T. Okuda, Y. Okimoto, R. Kumai, K.-I. Kobayashi, and Y. Tokura, Phys. Rev. B **61**, 422 (2000).
[15] T. Okuda, A. Asamitsu, Y. Tomioka, T. Kimura, Y. Taguchi, and Y. Tokura, Phys. Rev. Lett. **81**, 3203 (1998).
[16] Y. Okimoto, T. Katsufuji, T. Ishikawa, A. Urushibara, T. Arima, and Y. Tokura, Phys. Rev. Lett. **75**, 109 (1995).